

Preparation of Amorphous Metal-Oxide-Core Polymer-Shell Nanoparticles via a Microemulsion-Based Sol–Gel Approach

Dieter Holzinger and Guido Kickelbick*

Institut für Materialchemie, Technische Universität Wien, Getreidemarkt 9, A1060 Wien, Austria

Received April 8, 2003. Revised Manuscript Received September 22, 2003

A general route toward surface-functionalized amorphous metal oxide nanoparticles via a sol–gel approach is presented. Modified metal alkoxides were obtained by the substitution of alkoxide groups against functionalized pentane-2,4-dione derivatives, which had potential initiating sites for atom transfer radical polymerization (ATRP). Surface-modified amorphous metal oxide nanoparticles of titanium, zirconium, tantalum, yttrium, and vanadium were synthesized using these novel precursors in a microemulsion-based sol–gel process. Particles with diameters below 200 nm were prepared, and the resulting surface-functionalized colloids were used as macroinitiators in ATRP reactions. The combination of the two well controllable processes, i.e., microemulsions for the formation of the inorganic core and ATRP for the polymer shell, allows for the good control over the composition and morphology of these core–shell systems.

Introduction

Inorganic–organic core–shell nanoparticles have recently gathered a lot of scientific interest due to the possibility to combine different properties of core and shell in one particle.¹ In addition, many interesting technological applications are under development for this kind of materials, for example in analytical chemistry (chromatography), separation technology (ion exchange), catalysis, biochemistry, and medicine, etc.^{2,3} Core–shell systems with silica cores are well-established materials, but appropriate general routes for such morphologies with transition metal oxide cores are still rare.

A prominent mild method for the formation of metal oxide materials is the hydrolysis of metal alkoxides in a sol–gel reaction. This approach was already used by Stöber in 1968 for the preparation of silica nanoparticles.⁴ The adaptation of the latter technique has allowed the formation of organically surface-functionalized silica colloids.^{5–7} However, the usual employed conditions for this method, i.e., hydrolysis of metal alkoxides in a solvent such as an alcohol by addition of water, are not suitable for the controlled preparation of transition metal oxide nanoparticles because of the

fast hydrolysis and condensation rates of their alkoxides. Furthermore, contrary to the surface modification of silica nanoparticles where silane-coupling agents with hydrolytically stable Si–C bonds are used, a controlled modification of the surface of transition metal oxide colloids often requires different, such as coordinative, interactions.

A controlled method to prepare metal oxide nanoparticles via the sol–gel route is the use of a water-in-oil emulsion in which the stabilized aqueous micelles act as a kind of nanoreactor.^{8–10} However, most of the literature-described particles prepared via this technique had no additional surface functionality except the residues of alkoxide groups or adsorbed surfactants. Recently, ligand-stabilized crystalline nanoparticles of titania^{11–13} and tin oxide¹⁴ were obtained at 60 °C. However, if, for example, thermally unstable polymerization initiators for free radical polymerization should be immobilized on the surface of the particles lower temperatures are necessary.

In this work we describe a general route for the synthesis of inorganic–organic particles consisting of an amorphous metal oxide core and a polymeric shell via the combination of molecular precursor design, microemulsion approach, and surface grafting of polymers.

* To whom correspondence should be addressed. Fax: +43-1-58801-15399. E-mail: guido.kickelbick@tuwien.ac.at.

(1) Caruso, F. *Adv. Mater.* **2001**, *13*, 11.
(2) Zhong, C.-J.; Maye, M. M. *Adv. Mater.* **2001**, *13*, 1507.
(3) Bourgeat-Lami, E. *J. Nanosci. Nanotech.* **2002**, *2*, 1.
(4) Stöber, W.; Fink, A.; Bohn, E. *J. Colloid Interface Sci.* **1968**, *26*, 62.
(5) Philipse, A. P.; Vrij, A. *J. Colloid Interface Sci.* **1989**, *128*, 121.
(6) Beck, C.; Hartl, W.; Hempelmann, R. *Angew. Chem., Int. Ed.* **1999**, *38*, 1297.
(7) Tolnai, G.; Csempesz, F.; Kabai-Faix, M.; Kalman, E.; Keresztes, Z.; Kovacs, A. L.; Ramsden, J. J.; Horvoelgyi, Z. *Langmuir* **2001**, *17*, 2683.

(8) Meyer, F.; Hempelmann, R.; Mathur, S.; Veith, M. *J. Mater. Chem.* **1999**, *9*, 1755.
(9) Zarur, A. J.; Hwu, H. H.; Ying, J. Y. *Langmuir* **2000**, *16*, 3042.
(10) Tartaj, P.; De Jonghe, L. C. *J. Mater. Chem.* **2000**, *10*, 2786.
(11) Scolan, E.; Sanchez, C. *Chem. Mater.* **1998**, *10*, 3217.
(12) Scolan, E.; Magnenet, C.; Massiot, D.; Sanchez, C. *J. Mater. Chem.* **1999**, *9*, 2467.
(13) Roux, S.; Soler-Illia, G. J. A. A.; Demoustier-Champagne, S.; Audebert, P.; Sanchez, C. *Adv. Mater.* **2003**, *15*, 217.
(14) de Monredon, S.; Cellot, A.; Ribot, F.; Sanchez, C.; Armelao, L.; Gueneau, L.; Delattre, L. *J. Mater. Chem.* **2002**, *12*, 2396.

Experimental Section

Measurements. NMR spectra were recorded on a 300 MHz DRX Avance Bruker or Bruker AC 250 instrument working at 300 (250) and 75.43 (66.9) MHz for ^1H and ^{13}C , respectively. Relative size exclusion chromatography (SEC) measurements in THF were performed using a Waters system including a Waters 515 HPLC pump, a Waters 717 autosampler, a Waters 2410 differential refractive index detector, and Styragel columns (HR 0.5, 3, and 4, linear) at 40 °C at a rate of 1 mL/min applying linear polystyrene standards. Molecular weight analysis was calculated with Waters Millennium³² software including the GPC/V option and related to an internal standard (diphenyl ether). Dynamic light scattering (DLS) measurements were performed applying a noninvasive backscattering technique by using an ALV-NIBS/HPPS instrument and determination of the particle diameter via distribution function and cumulant analyses. TEM measurements were performed on a JEOL JEM-200CX instrument. IR measurements for solid samples were carried out with a Perkin-Elmer 16PC FT-IR instrument and with a Biorad FTS 135 instrument for liquid samples. Thermal gravimetric analyses were carried out on a Shimadzu TG-50 instrument with a heating rate of 5 °C/min. Microanalyses were carried out by the Microanalytical Laboratories, University of Vienna.

Materials. Fe(OEt)₃ was obtained from Vadim Kessler, Department of Chemistry, SLU, Uppsala, Sweden. All other chemicals were obtained from Sigma-Aldrich and Gelest. CuBr and CuCl were stirred in glacial acetic acid overnight, filtered, and washed with absolute ethanol. Monomers were distilled from CaH₂, degassed, and stored in a refrigerator prior to use. All other chemicals were used without further purification. All reactions in which metal alkoxides were used (with exception of the microemulsions) were carried out under an argon atmosphere using Schlenk techniques.

Syntheses. *3-Bromopentane-2,4-dione (2)*. Pentane-2,4-dione (10.1 g; 0.101 mol), 60 mL of distilled water, and 60 mL of chloroform were mixed and cooled below 0 °C. A mixture of 16.2 g (0.101 mol) of bromine and 40 mL of chloroform was added dropwise within 1 h under vigorous stirring. The stirring was continued for an additional hour. After drying of the organic layer with MgSO₄ the chloroform was removed in vacuo. Yield: 15.06 g (83.3%). Elemental analyses: calc. 33.6% C, 3.9% H, 44.6% Br; found 33.2% C, 4.2% H, 42.3% Br. ^1H NMR (δ , CDCl₃, 22 °C): 2.22 (m, 3H, CH₃-CO) ppm. ^{13}C NMR (δ , CDCl₃, 22 °C): 190.1 (CO), 100.7 (COCCO), 27.6 (CH₃-CO) ppm. IR (ν , chloroform): 1717 (keto CO), 1599 (enol CO) cm⁻¹.

3-(2-Bromo-2-methylpropylidene)pentane-2,4-dione (3). To a mixture of 8.00 g (0.053 mol) of 2-bromo-2-methylpropanal and 5.30 g (0.053 mol) of pentane-2,4-dione, 45 mg (0.053 mol) of piperidine was added. The solution was stirred for 30 min and afterward deposited in the refrigerator for 48 h. The solution was extracted with a mixture of 100 mL of chloroform and 100 mL of 5% HCl. The organic phase was dried with MgSO₄ and the solvent was removed in vacuo. Yield: 5.3 g (42.74%). Elemental analyses: calc. 46.37% C, 5.62% H; found 43.7% C, 5.6% H. ^1H NMR (δ , CDCl₃, 22 °C): 7.22 (s, 1H, CH), 1.97 (s, 6H, (CH₃)₂-CBr), 1.74 (CH₃-CO) ppm. ^{13}C NMR (δ , CDCl₃, 22 °C): 192.7 (CH₃-CO-C), 104.2 (CO-C-CO), 85.7 (CH), 68.1 ((CH₃)₂C(CH)Br), 25.5 ((CH₃)₂C), 25.1 (CH₃-CO-C) ppm. IR (ν , chloroform): 1725 (keto CO), 1620 (enol CO) cm⁻¹.

1-Acetyl-2-oxopropyl 2-bromo-2-methylpropanoate (4). 2-Bromo-2-methylpropionic acid (3.34 g; 0.02 mol) and 6.79 g (0.02 mol) of (N(Bu)₄)HSO₄ as phase transfer catalyst were dissolved in 10 mL of 2 M NaOH and stirred for 30 min. The solution was extracted 3× with 30 mL of dichloromethane and the combined organic phases were dried with MgSO₄. After filtration 4.04 g (0.03 mol) of 2-chloro-pentane-2,4-dione was added and the mixture was refluxed overnight. Afterward the solution was washed 3× with 20 mL of 2.5 M H₂SO₄ and 20 mL of water and dried with MgSO₄, and the solvent was removed in vacuo. Yield: 4.15 g (78.3%). Elemental analyses: calc. 40.78% C, 4.94% H; found 42.4% C, 5.7% H. ^1H NMR (δ , CDCl₃, 22 °C): 2.10 (m, 6H, CH₃-CO), 1.97 (m, 6H, CH₃-C)

ppm. ^{13}C NMR (δ , CDCl₃, 22 °C): 192.5 (CH₃-CO-C), 182.3 (O-CO-C) 111.6 (CO-C-CO), 62.6 (Br-C(CH₃)₂), 27.8 (Br-C(CH₃)₂), 23.4 (CH₃-CO) ppm. IR (ν , chloroform): 1730 (keto CO), 1601 (enol CO) cm⁻¹.

3-Acetyl-5-bromo-5-methylhexane-2,4-dione (5). Pentane-2,4-dione (8.00 g; 0.08 mol), 18.37 g (0.08 mol) of 2-bromo-2-methylpropanoyl bromide, and 11.04 g (0.08 mol) of K₂CO₃ were stirred in 80 mL of absolute acetone overnight and the acetone was removed in vacuo. Yield: 15.35 g (77.1%). Elemental analyses: calc. 43.39% C, 5.26% H; found 42.9% C, 5.3% H. ^1H NMR (δ , CDCl₃, 22 °C): 2.10 (m, 6H, CH₃-CO), 1.97 (m, 6H, CH₃-C); ^{13}C NMR (δ , CDCl₃, 22 °C): 188.5 (CH₃-CO-C), 177.6 (CH-CO-C), 100.8 (C(CO)₂), 30.9 ((CH₃)₂C-Br), 25.2 (CH₃-CO-C) ppm. IR (ν , chloroform): 1730 (keto CO), 1609 (enol CO) cm⁻¹.

General Procedure for the Coordination of the Pentane-2,4-dione Derivatives to the Metal Alkoxide. All pentane-2,4-dione derivatives were reacted in a 1:1 ratio with the metal alkoxides under an argon atmosphere. 3-Chloro- (1) and 3-bromo-pentane-2,4-dione (2) were reacted with the metal alkoxide by stirring them at 0 °C without a solvent. The precipitate was used without further purification. All other pentane-2,4-dione derivatives were mixed with the metal alkoxides and refluxed overnight in absolute toluene. The solvent was evaporated in vacuo, and the product was used without further purification in the microemulsion reactions. The coordination of the bidentate ligands to the metal alkoxides was proved via IR spectroscopy. The following list contains the results for the coordination of the ligands to Ti(O^{*i*}Pr)₄. IR (ν , chloroform): (1) 1576 (CO coord.), (2) 1713 (CO keto), 1568 (CO coord.), (3) 1725 (CO keto), 1593 (CO coord.), (4) 1576 (CO coord.), (5) 1730 (CO keto), 1582 (CO coord.) cm⁻¹. Similar absorption bands were observed for the other metal alkoxides.

Nanoparticle Formation in Microemulsions.¹⁵ Cyclohexane (14.50 g; 58 wt %) was mixed with 3.75 g (15 wt %) of *n*-hexanol and 4.75 g (19 wt %) of Triton X-100 and stirred for 5 min. Afterward 2.00 g (8 wt %) of water was added and stirred for 20 min. Under vigorous stirring, the modified alkoxide (0.25 g) was added and stirred overnight. The nanoparticles were centrifuged and washed with a mixture of chloroform and methanol, and toluene.

Coordination of the pentane-2,4-dione derivatives to the titania particles was proved via IR spectroscopy. IR (ν , chloroform): (1) 1576 (CO coord.), (2) 1568 (CO coord.), (3) 1593 (CO coord.), (4) 1576 (CO coord.), (5) 1582 (CO coord.) cm⁻¹.

Polymerizations. All polymerizations were carried out following standard procedures for atom transfer radical polymerizations.¹⁶

Cleavage of Polystyrene from the Inorganic Particle Core. A 100-mg portion of polystyrene-modified titania particles was suspended in 10 mL of concentrated NaOH solution and the suspension was stirred for 3 d at room temperature. The polymer was filtered, washed several times with water, and dried in vacuo before the samples were analyzed by NMR and SEC.

Results and Discussion

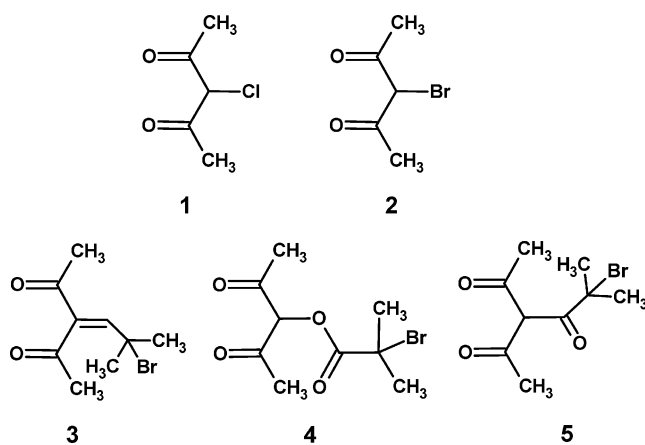
Precursor Formation. The fast hydrolysis rate of metal alkoxides compared to silicon alkoxide can be decreased by the coordination of bidentate ligands. One example is the use of functionalized carboxylic acids that proved already their applicability as ligands in the synthesis of sub-nanometer sized surface-modified metal oxo clusters of titanium, zirconium, vanadium, and other metals.¹⁷ The carboxylic acids act as bridging or chelating ligands in these compounds. Pentane-2,4-dione, as another example of a bidentate ligand, was

(15) Chhabra, V.; Pillai, V.; Mishra, B. K.; Morrone, A.; Shah, D. O. *Langmuir* **1995**, *11*, 3307.

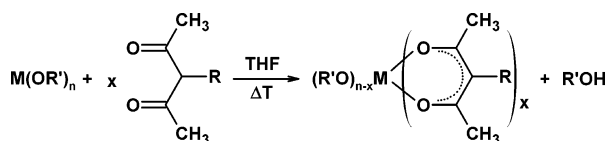
(16) Xia, J.; Matyjaszewski, K. *Macromolecules* **1997**, *30*, 7697.

(17) Kickelbick, G.; Schubert, U. *Monatsh. Chem.* **2001**, *132*, 13.

Scheme 1



Scheme 2



already used for a reduction of the reaction rate of metal alkoxides in the sol-gel process and therefore it allows for a better control in the formation of the colloidal particles as well.^{11,18} An additional advantage of this ligand is its rather simple functionalization in the 3-position via deprotonation and C-C bond formation.¹⁹ We are particularly interested in the controlled grafting of polymers from the surface of metal oxide particles for the preparation of inorganic-core polymeric-shell nanoparticles. Therefore, pentane-2,4-dione was modified with initiating groups for atom transfer radical polymerization (ATRP). Modified pentane-2,4-dione derivatives used in this work are shown in Scheme 1. All these compounds contain C-X bonds (X = Cl, Br) that can be homolytically cleaved throughout ATRP and which are able to initiate this polymerization.

An interesting detail of these compounds is the dependence of the keto-enol ratio on the substitution pattern in the 3-position, which has a direct impact on the reactivity of the modified bidentate ligands toward substitution reactions of metal alkoxides. A qualitative study of the ratios between the two isomeric forms of the pure diketones was carried out via IR spectroscopy. While the ligands (2) and (3) exist primarily as diketones, compound (1) exists exclusively in its enol form, and the compounds (4) and (5) appear in both forms.

The obtained pentane-2,4-dione derivatives were coordinated to various metal alkoxides by a ligand exchange reaction, which resulted in pentane-2,4-dionate-substituted alkoxides (Scheme 2).²⁰ In principle all available metal alkoxides that allow a substitution of the alkoxide can be used in this reaction, for first studies of the general applicability of this method we produced bidentate ligand substituted alkoxides from Ti(OⁱPr)₄, Zr(OⁿBu)₄, Fe(OEt)₃, Ta(OEt)₅, Y(OⁱPr)₃, and VO(OEt)₃.

Ti(OⁱPr)₄ and Zr(OⁿBu)₄ were exemplarily substituted with all synthesized ligands and the products were characterized via IR and NMR spectroscopy. All other alkoxides were only reacted with compound (4).

In the cases of the ligands (1) and (4) a 1:1 substitution was achieved with Ti(OⁱPr)₄ and the coordination was verified via IR and NMR spectroscopy. The absorption band of the keto form at 1717 and 1730 cm⁻¹ disappeared after coordination and a new band at 1576 cm⁻¹ emerged, which is consistent with the formation of a coordinated pentane-2,4-diketonate. The absorption band of the keto form of compound (5) with three potential coordinating sites did not disappear completely because not all three keto groups coordinated to the metal. A complete coordination of substance (2) and (3) was not possible even after longer reaction times, therefore absorption bands at 1713 cm⁻¹ and 1725 cm⁻¹ remained and new bands at 1568 and 1593 cm⁻¹ were detected. This is a strong indication for the presence of free or only weakly coordinated diketones or enols in these cases. The NMR spectra of the resulting compounds were complex and no distinct assignment of the peaks could be carried out. One of the possible reasons for the difficulty in assigning the signals is that only mixtures of different substitution products (single- and double-substituted with pentane-2,4-derivatives) can be obtained. A further purification and separation of the products was not necessary because the obtained mixture of coordination compounds could already be used as a precursor for the sol-gel process in the microemulsion.

Particle Formation. The substituted alkoxides were used as precursors for the sol-gel process in a water-in-oil microemulsion with cyclohexane as the continuous phase, the commercially available Triton-X100 as a nonionic surfactant, and 1-hexanol as a cosurfactant. In all reactions the amount of metal alkoxide and the water-to-alkoxide ratio in the microemulsion was kept constant. The size of the obtained amorphous metal oxide particles was strongly influenced by the reaction time. A comparison of the normalized particle diameter growth, as analyzed by dynamic light scattering (DLS), of titanium isopropoxide and zirconium butoxide modified with ligand (1), and titanium isopropoxide modified with compound (4) (microemulsion process), with the growth of unmodified SiO₂ particles obtained in the Stöber process is shown in Figure 1. The pentane-2,4-diketonate-substituted metal alkoxides with an organic substituent in the 3-position reacted with a rate comparable to that of the silicon alkoxides in the Stöber process, whereas the halogen-substituted systems revealed a slower particle growth. The reason for this behavior might be a result of the electronic structure of the latter ligands containing an electron-withdrawing atom in the 3-position and its influence on the hydrolysis rate of the metal alkoxide. Although differences of the reaction kinetics were observed, all obtained nanoparticles revealed a rather monodisperse size distribution as determined via DLS measurements. Figure 2 shows the TEM images of the organically surface-modified amorphous nanoparticles obtained under the same reaction conditions of (a) titania (diameter 175 nm), (b) vanadium oxide (diameter 25 nm), (c) yttrium oxide (diameter 100 nm), (d) zirconium oxide (diameter

(18) Leautic, A.; Babonneau, F.; Livage, J. *Chem. Mater.* **1989**, *1*, 248.

(19) Cativiela, C.; Serrano, J. L.; Zurbano, M. M. *J. Org. Chem.* **1995**, *60*, 3074.

(20) Leautic, A.; Babonneau, F.; Livage, J. *Chem. Mater.* **1989**, *1*, 240.

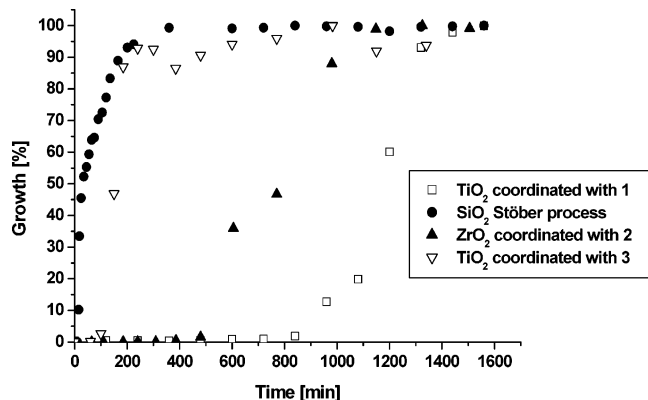


Figure 1. Comparison of the kinetic of the particle growth between Stober particles (SiO_2) (3.9 g (1.88×10^{-2} mol) of TEOS in 120 mL of ethanol and 6 mL of NH_3 (25%) at room temperature) and metal alkoxide pentane-2,4-dione derivatives which were used in a microemulsion process (58 g of cyclohexane, 15 g of hexanol, 19 g of Triton-X100, 8 g of water; 1 g of acetylacetonate-substituted metal alkoxide; pH = 6; at room temperature).

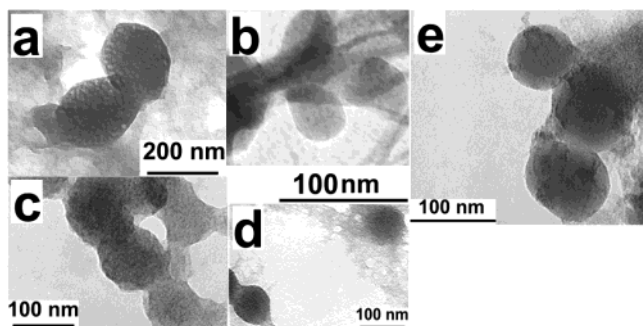


Figure 2. TEM images of surface-modified nanoparticles of (a) amorphous titania, (b) vanadium oxide, (c) yttrium oxide, (d) zirconium oxide, and (e) iron oxide.

80 nm), and (e) iron oxide (diameter 100 nm). The TEM images reveal that the growth of the nanoparticles occurred in different ways; for example, in the case of titania (Figure 2a) the final surface-modified particle is formed by an agglomerate of smaller colloids, whereas other metal oxides formed more homogeneous products. This observation can be ascribed to different growing mechanisms in the micelles. The hydrolysis of some of the metal alkoxides seems to be so fast that several condensation centers are formed in the water droplet, and the final particle is the product of an agglomeration of smaller colloids. In other cases, the condensation reaction seems to be more homogeneous. In addition, the TEM images also show that the single particles form agglomerates on the support, which can be traced back to the absence of surface-charge usually observed in the case of unmodified inorganic particles that leads to repulsion of the single particles and the presence of attracting van der Waals forces between the organically modified particle surfaces. In contrast, no agglomeration was observed in diluted dispersions of the nanoparticles in ethanol as measured via DLS. Proof that the pentane-2,4-dione molecules are still attached to the particle surface are the typical absorption bands ($1560\text{--}1590\text{ cm}^{-1}$) which are still present in the FTIR spectra of the isolated and purified samples.

Thermal gravimetric analysis allowed the estimation of the overall organic content of the particles and an

estimation of the halogen content on the surface using the approximation that all bidentate ligands are attached to the surface. However, it cannot be excluded that partially alkoxide groups or bidentate ligands are located in the core of the particles. This is probably the reason the resulting values differ from elemental analyses where the halogen content was systematically lower. The obtained concentration of halogen atoms was calculated to be between 0.6 and 1.0 mmol per g of nanoparticle depending on the functional group and the metal alkoxide used. These values are comparable with the results of Van Blaaderen and Vrij who functionalized SiO_2 nanoparticles with much less sterically demanding silane coupling agents, such as methacryloxypropyltrimethoxysilane, for which they obtained 1.56 mmol per g.²¹ Temperature-dependent mass spectroscopic measurements showed that there are still alkoxide substituents on the surface of the nanoparticles which are removed at much lower temperatures (usually below $100\text{ }^\circ\text{C}$) than the pentane-2,4-diketone derivatives (higher than $150\text{ }^\circ\text{C}$). The prepared and isolated nanoparticles were also characterized via IR spectroscopy. No differences compared to the signals of the molecular precursors were observed, which proves that the initiating groups were incorporated in the particles or at the particle surface.

Polymerizations. The resulting surface-functionalized particles were used as multifunctional initiators for ATRP with methyl methacrylate (MMA) and styrene as monomers. ATRP allows, contrary to conventional free radical polymerizations, the exclusive grafting of the polymer chain from the particle surface. In addition, the polymerization reaction is usually controlled, which means that the chain length and therefore the polymer layer thickness can be adjusted nicely. ATRP already showed its potential in the surface-modification of silica nanoparticles.^{22,23} In addition to the above-mentioned facts concerning ATRP, the use of the modified nanoparticles as multifunctional initiators also proves that the initiating groups are located at the surface of the colloids because only there a polymerization can be initiated. Unmodified nanoparticles did not initiate the polymerization, which was proved experimentally.

Kinetic studies were carried out using NMR to investigate whether the polymerization shows the typical first order kinetics concerning the monomer concentration, which is usually observed for controlled polymerizations such as ATRP. As an example, the kinetics of a MMA polymerization initiated by 5-bromo-5-methyl-3-oxoethylhexane-2,4-dione-modified TiO_2 nanoparticles of 80-nm diameter is shown in Figure 3. The $\ln([M]_0/[M])$ vs time plot reveals the typical linear dependence of a controlled/"living" polymerization. Furthermore, in the case of a controlled polymerization, the particle radius should also change linearly by time if we take into account that all polymer chains grow with the same speed and termination reactions only rarely occur. The particle radius of the investigated grafting from polymerization from the surface of the titania particles was studied by DLS in a THF solution. Although the particle

(21) Blaaderen, A. v.; Vrij, A. *J. Colloid Interface Sci.* **1993**, *156*, 1.

(22) Von Werne, T.; Patten, T. E. *J. Am. Chem. Soc.* **1999**, *121*, 7409.

(23) Pyun, J.; Matyjaszewski, K.; Kowalewski, T.; Savin, D.; Patter-son, G.; Kickelbick, G.; Hüsing, N. *J. Am. Chem. Soc.* **2001**, *123*, 9445.

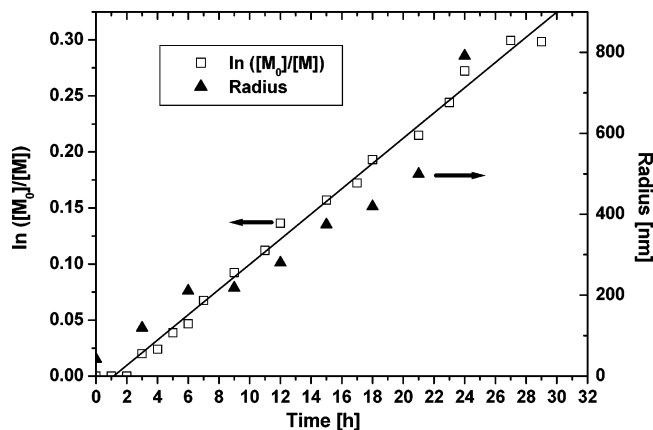


Figure 3. Kinetics of an ATRP initiated by 5-bromo-5-methyl-3-oxoethylhexane-2,4-dione-modified TiO_2 nanoparticles with MMA as monomer in 6 mL of toluene. Conditions: 140 mg of nanoparticles, $\text{CuCl/pmdeta/MMA} = (1.99 \times 10^{-3}/1.99 \times 10^{-3}/9.99 \times 10^{-2})$ mol, 90 °C (pmdeta = *N,N,N',N'*-pentamethylethylenetriamine).

radius probably cannot be directly correlated with the extended chain length, due to the measurement limits of DLS (assumption of spherical particles, swelling of the polymer shell in the solvent), it gives a rough estimation of the trend of the particle growth. A linear dependence of the particle radius with reaction time was observed (Figure 3).

A study of the polymers grafted from the surface of the titania particles by conventional polymer characterization techniques (SEC, NMR) was carried out by dissolving the particle core in concentrated NaOH in an ultrasound bath. The analysis of the molecular weights therefore needs to be treated with caution. SEC resulted for the polystyrene polymers at 14% conversion in a molecular weight of 148 000 g/mol and a molecular weight distribution of 1.4, and the polymerization of MMA under the same conditions led to a molecular weight of the polymer of 97 500 g/mol and a polydispersity of 1.87 at 21% conversion. These results show that the grafting of the polymers seems to be not controlled, which can be a result of the closeness of initiating groups on the surface that can lead to termination reactions. In addition, a total dissolving of the inorganic core cannot be guaranteed, because of the good protection of the inorganic core by the organic shell and the more difficult dissolving of titania as compared to other inorganic oxides, such as silica. For future investigations, other possibilities have to be investigated for the cleavage of the polymers from the inorganic core, such as the introduction of labile organic groups in the initiating molecule to get a trustable result of the polymer analysis.

The final polymer-capped core-shell titania nanoparticles were characterized via TEM, but the polymers

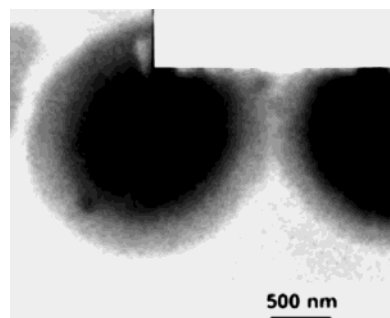


Figure 4. Core-shell nanoparticles with an amorphous titania core of 1.2 μm diameter and a PMMA shell with a thickness of 400 nm.

of the smaller particles decomposed in the electron beam. However, to prove the core-shell nature of the particles we synthesized larger micrometer-sized particles as model systems with the same methodology as described above. Figure 4 shows a TEM image of a model particle consisting of an amorphous titania core and a PMMA shell.

Conclusions

We presented a novel general approach for the synthesis of inorganic-organic core-shell nanoparticles. Applying the microemulsion technique allows the use of transition metal alkoxides and guarantees a narrow size distribution. Modifying the alkoxides with initiators resulted in nanoparticles with polymerizable groups on the surface that allowed for a polymerization from the surface ("grafting from"). Depending on the chosen microemulsion composition a wide range of different nanoparticles was prepared containing various functionalizations coordinated to the surface. The resulting macroinitiators were used in ATRP which allowed for very good control over the diameter of the resulting inorganic-organic core-shell nanoparticles. Hence, by using microemulsions for the synthesis of the inorganic core and ATRP for the preparation of the polymer shell an overall control of the particle composition and morphology was obtained.

Acknowledgment. We thank Dr. Nicola Söger from the Institute of Inorganic Chemistry, University of Hanover, Germany, for technical assistance with the temperature-dependent mass spectroscopic measurements. We gratefully acknowledge the financial support by the Fonds zur Förderung der wissenschaftlichen Forschung Austria. We thank Prof. Vadim Kessler, Department of Chemistry, SLU, Uppsala, Sweden for providing us with $\text{Fe}(\text{OEt})_3$.

CM031068R